



# Evaluating the impacts of fishing and migratory species in a temperate bay of China using the ecosystem model OSMOSE-JZB

Lei Xing, Yong Chen, Robert Boenish, Kisei R. Tanaka, Nicolas Barrier,  
Yiping Ren

## ► To cite this version:

Lei Xing, Yong Chen, Robert Boenish, Kisei R. Tanaka, Nicolas Barrier, et al.. Evaluating the impacts of fishing and migratory species in a temperate bay of China using the ecosystem model OSMOSE-JZB. Fisheries Research, 2021, 243, pp.106051. 10.1016/j.fishres.2021.106051 . hal-03415714

**HAL Id: hal-03415714**

**<https://hal.umontpellier.fr/hal-03415714>**

Submitted on 27 Mar 2023

**HAL** is a multi-disciplinary open access archive for the deposit and dissemination of scientific research documents, whether they are published or not. The documents may come from teaching and research institutions in France or abroad, or from public or private research centers.

L'archive ouverte pluridisciplinaire **HAL**, est destinée au dépôt et à la diffusion de documents scientifiques de niveau recherche, publiés ou non, émanant des établissements d'enseignement et de recherche français ou étrangers, des laboratoires publics ou privés.



Distributed under a Creative Commons Attribution - NonCommercial 4.0 International License

# Evaluating the impacts of fishing and migratory species in a temperate bay of China using the ecosystem model OSMOSE-JZB

Lei Xing<sup>a,b</sup>, Yong Chen<sup>b,c</sup>, Robert Boenish<sup>d</sup>, Kisei R. Tanaka<sup>e</sup>, Nicolas Barrier<sup>f</sup>, Yiping Ren<sup>a,c,\*</sup>

<sup>a</sup> College of Fisheries, Ocean University of China, Qingdao 266003, China

<sup>b</sup> School of Marine Sciences, University of Maine, Orono, ME, 04469, USA

<sup>c</sup> Laboratory for Marine Fisheries Science and Food Production Processes, Pilot National Laboratory for Marine Science and Technology (Qingdao), Qingdao 266237, China

<sup>d</sup> 1019 East Capitol St. SE, Washington, DC 20003, USA

<sup>e</sup> Pacific Islands Fisheries Science Center, National Oceanic and Atmospheric Administration, Honolulu, HI, 96815, USA

<sup>f</sup> MARBEC, Univ. Montpellier, CNRS, Ifremer, IRD, S'ete, France

Small-scale fisheries (SSFs) play a vital role in the sustainability of local economies. Migratory species moving into and out of an ecosystem may influence the dynamics of local fish communities and SSFs. We used the end-to-end model, OSMOSE-JZB (Object-oriented Simulator of Marine ecOSystEms), to evaluate the impacts of fishing and a migratory shrimp (*Trachypenaeus curvirostris*) on the ecosystem of Jiaozhou Bay, China. Increased fishing intensity (i.e., annual fishing effort) resulted in the decline of four ecological indicators, including the total biomass of the community, mean trophic level of the community, inverse fishing pressure, and large fish index. Compared to managing fish stocks under uniform fishing mortality over the fishing season, landings and community biomass were higher when a “race to fish” (i.e., large catches in a short period) occurred. The results suggested that managing fishing seasonality (i.e., temporal allocation of fishing effort) could mitigate the negative impact of fishing intensity. Two resident high-trophic-level fishes were sensitive to changes in fishing intensity and fishing seasonality. The changes in trophic interactions had larger impacts on species at low trophic levels than fishing. Pearson’s correlation analysis showed that *T. curvirostris* biomass was negatively correlated with the biomass of resident species and positively correlated with the biomass of other migratory species. We also found that fishing changed the impact of varying *T. curvirostris* migratory biomass on other species. Resident species were more sensitive to changes in fishing and *T. curvirostris* migratory biomass than other migratory species. We argue that SSFs management can benefit from the development of temporal fishing strategies and consideration of trophic interactions stemming from migratory species dynamics.

## 1. Introduction

Small-scale fisheries (SSFs) constitute an important source of global fisheries landings, employ millions of people, and support food and nutrient security for more than a billion people (Food and Agriculture Organisation (FAO), 2018). SSFs have been increasingly recognized for their significant socio-economic importance to the local economy and development (Teh and Sumaila, 2013; Said and Chuenpagdee, 2019). Concerns about the viability and sustainability of SSFs have grown in recent years (Salas et al., 2019). The multispecies and multigear nature of SSFs requires managing fish stocks at an ecosystem level (Herrón

et al., 2019). SSFs management remains less well studied compared to large-scale industrial fisheries. Data limitations impede sound stock assessment and decision-making processes for SSFs management (Ramírez et al., 2017).

Overfishing threatens the sustainable development of SSFs (Gough et al., 2020). Fishermen’s behaviors are inextricably tied to stock status (Kiyama and Yamazaki, 2018). The importance of understanding the behavioral response of fishermen to varying resource conditions is becoming widely recognized for achieving sustainable management (Fulton et al., 2011). Large-scale environmental changes not only influence spatio-temporal variations in natural resources and fishery

\* Corresponding author at: Room 2216 Fisheries Hall, 5 Yushan Road, Qingdao, China.

E-mail addresses: xinglei0726@126.com (L. Xing), ychen@maine.edu (Y. Chen), robert.boenish@gmail.com (R. Boenish), kisei.tanaka@noaa.gov (K.R. Tanaka), nicolas.barrier@ird.fr (N. Barrier), renyip@ouc.edu.cn (Y. Ren).

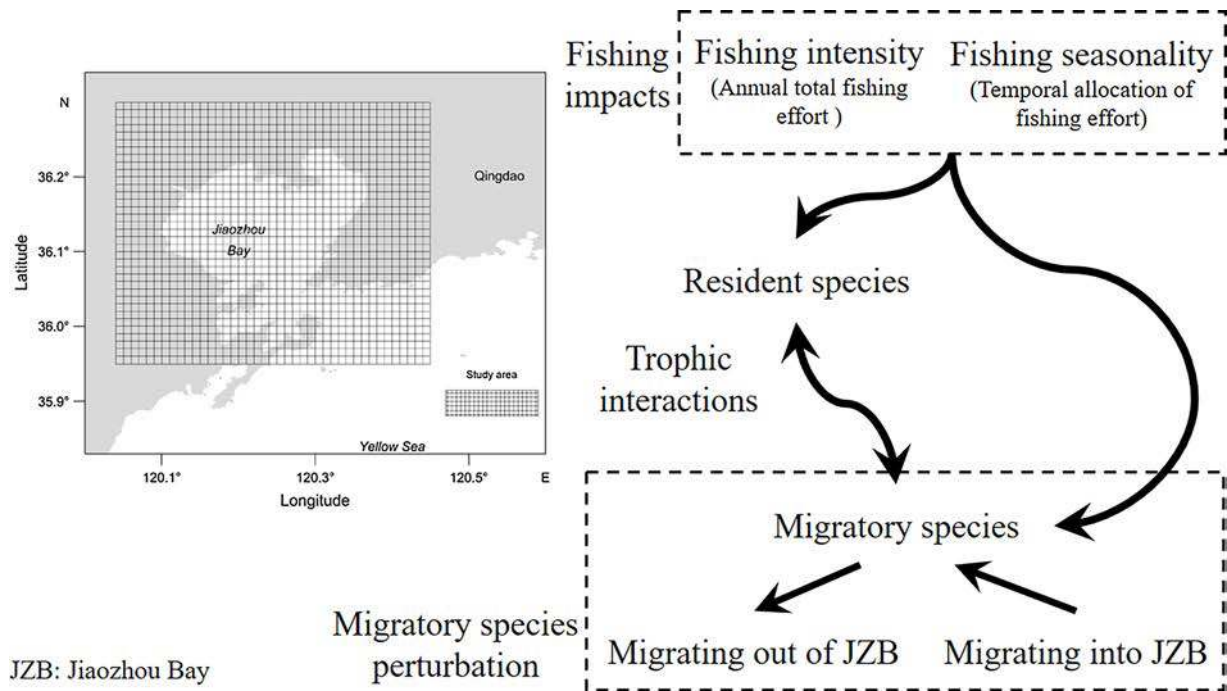


**Fig. 1.** Impacts of fishing and migratory species in Jiaozhou Bay, China (JZB). A grid map of the study area is shown on the left.

productivity (Moullec et al., 2019) but also systematically increase uncertainty for SSFs management (Finkbeiner et al., 2018). Some work has suggested that changes in migratory species biomass may alter the stability of local ecosystems (Mormul et al., 2012; Stockwell et al., 2014). Shifts in ecosystem function further challenge the competing goals of balancing the short-term needs and long-term conservation of natural resources in SSFs management.

Marine ecosystems are becoming fragile as a result of decadal overfishing (Pauly and Liang, 2019). China's central government and provincial governments have implemented management tools to mitigate harmful fishing impacts in the last decade, including marine protected areas (MPAs), a summer fishing moratorium, and minimum mesh size regulations (Su et al., 2020). Nonetheless, reports of depleted fish stocks have increased in recent years, and species at lower trophic levels are becoming more dominant in Chinese coastal waters (Szuwalski et al., 2017). Fishermen often exhibit a "race to fish" behavior where substantial fishing effort is concentrated immediately following a seasonal fishing closure or during a spawning season (Wang, 2014; Sys et al., 2017). The warming climate influences migratory fish stocks, such as *Trichiurus japonicus* and *Larimichthys polyactis* (Yuan et al., 2017). These factors further complicate the management of SSFs, which greatly depend on local fish stocks.

China's government launched the "Blue Granary" concept aiming to safeguard food security in China (Yang, 2019). Ecosystem-based fisheries management (EBFM) is emphasized as a national direction and pathway for fisheries management. EBFM seeks a broadening consideration of trade-offs between managing fisheries for socio-economic profit and ecosystem stability (Pikitch et al., 2004). Ecosystem modeling approaches are recognized as a necessary complement to single-species modeling approaches in moving towards EBFM (Hilborn, 2011). Ecosystem models, such as Ecopath and size-spectrum model, have been used to advise Chinese fisheries management (Zhang et al., 2016; Zhang Chen, et al., 2018; Zhang Fan, et al., 2018; Dai et al., 2020). To date, few studies have examined how variations in the temporal allocation of fishing effort and migratory species biomass influence the conservation of natural resources at an ecosystem level (Chen et al., 2019).

In this study, we simulated a small-scale mixed species fishery in

Jiaozhou Bay, China. Jiaozhou Bay is a semi-enclosed bay located in the southeastern Shandong Peninsula, China. The fish community structure in Jiaozhou Bay has markedly shifted from large demersal species to small pelagic species (Ma et al., 2018). As a remediation strategy, a seasonal fishing closure has been implemented for many years (Wang, 2013), but it has been ineffective in avoiding further depletion (Zhu, 2009). Apart from seasonal fishing closures, there are few regulations governing the temporal allocation of fishing effort. The biomass of species that migrate into and out of Jiaozhou Bay has also shown changes in ecosystem productivity (Xu et al., 2019).

We used the end-to-end model, OSMOSE-JZB (Object-oriented Simulator of Marine ecOSystEms, OSMOSE), which was developed to simulate the full ecosystem dynamics of Jiaozhou Bay (Xing et al., 2017), as the operating model in our simulations. We address the following three issues regarding SSFs management in China: (1) impacts of variability in intensity and seasonality of fishing effort on fish stocks; (2) detection of species-specific responses to varying migratory species biomass; and (3) evaluation of the combined effect of fishing and migratory species on different species. We believe these issues have broad applicability in Chinese waters and beyond.

## 2. Materials and methods

### 2.1. Operating model: OSMOSE-JZB

OSMOSE-JZB is an application of the multispecies individual-based model OSMOSE that simulates the ecosystem dynamics of Jiaozhou Bay from plankton to top predators (Fig. 1). The modeled food web in OSMOSE-JZB contains low-trophic-level (LTL) and high-trophic-level (HTL) groups (Xing et al., 2017). The spatio-temporal distribution of LTL biomass is simulated by a biogeochemistry model, NEMURO (North Pacific Ecosystem Model Used for Regional Oceanography; Aita et al., 2007), coupled to an ocean physics model, FVCOM (Finite Volume Coastal Ocean Model; Chen et al., 2003). The OSMOSE model (Shin and Cury, 2001) simulates the full life cycle of HTL groups from egg to adult stages. The outputs of the FVCOM-NEMURO model are used to force the OSMOSE model. Spatio-temporal distributions of LTL biomass are used as prey fields to HTL groups. The LTL groups are classified as small

**Table 1**

Summary of high-trophic-level (HTL) groups modeled in the initial OSMOSE-JZB built by Xing et al. (2017).

| HTL group | Category            | Species (common name)   | Annual $M_{fishing}$ (Initial value) | Time steps for moving out of simulated domain |
|-----------|---------------------|---|--------------------------------------|---|
| SP0       | Mantis shrimp       | <i>Oratosquilla oratoria</i> (Japanese mantis shrimp)   | 0.420                                | Null  |
| SP1       | Small shrimp        | <i>Palaemon gravieri</i> (Chinese ditch prawn);<br><i>Parapenaeopsis tenella</i> (Smoothshell shrimp);<br><i>Alpheus japonicus</i> (Japanese snapping shrimp) | 0.365                                | Null  |
| SP2*      | Small crab          | <i>Charybdis bimaculata</i> (Two-spot swimming crab)  | 0.314                                | 0~5   |
| SP3*      | Large crab          | <i>Charybdis japonica</i> (Japanese swimming crab)  | 0.246                                | 0~11  |
| SP4*      | Loligo              | <i>Loligo</i> sp. (Squid)   | 0.419                                | 0~5   |
| SP5*      | Octopus             | <i>Octopus</i> sp. (Octopus)  | 0.350                                | Null  |
| SP6       | Large fish          | <i>Sebastes schlegelii</i> (Korean rockfish)  | 0.482                                | Null  |
| SP7*      | Small fish          | <i>Pholis fangi</i> (Gunnel)  | 0.426                                | 12~17   |
| SP8       | Small fish          | <i>Amblychaeturichthys hexanema</i> (Pinkgray gody)   | 0.229                                | Null  |
| SP9*      | Small fish          | <i>Thryssa kammalensis</i> (Kammal thryssa)   | 0.467                                | 0~5   |
| SP10*     | Large fish          | <i>Liparis tanakae</i> (Tanaka's snailfish)   | 0.488                                | 0~5; 12~17                                    |
| SP11      | Large fish          | <i>Johnius belangerii</i> (Belanger's croaker)  | 0.411                                | Null  |
| SP12*     | Medium-sized shrimp | <i>Trachypenaeus curvirostris</i> (Southern rough shrimp)   | 0.426                                | 0~11  |
| SP13      | Medium-sized fish   | <i>Cynoglossus joyneri</i> (Red tonguesole)   | 0.365                                | Null  |

Note: In a simulated year, there were 24 time steps numbered as 0–23. Migratory species were marked with \*. Annual  $M_{fishing}$  was the sum of fishing mortality rate at each time step. The annual  $M_{fishing}$  (initial value) was the same to that set in Xing et al. (2017). *Octopus* sp. (SP5\*) migrated out of Jiaozhou Bay at a given age. This HTL group occurred in the simulated domain all the year around. Therefore, its time steps for moving out of simulated domain was showed with null.

phytoplankton (PS), large phytoplankton (PL), small zooplankton (ZS), large zooplankton (ZL), and predatory zooplankton (ZP). The parameter *Plank.access* is used to calculate the proportion of available LTL biomass to HTL groups. As we focus on the impacts of fishing and migratory species on HTL groups, the configuration of FVCOM-NEMURO is not

presented in this study. A detailed description of our model can be found in Xing et al. (2017). Here, we briefly introduce the model structure and parameterization of the OSMOSE model.

The OSMOSE model is a multispecies individual-based model that simulates species life cycles and trophic interactions. The time step of the OSMOSE model is half of a month. The model is built based on data from four stratified random bottom trawl surveys conducted during 2011 in Jiaozhou Bay, China. There are 14 HTL groups modeled in the OSMOSE model, including 7 fishes, 2 crabs, 5 shrimp species, and 2 cephalopods (Table 1). Fish school is the basic modeling unit for each HTL group. There are six modeled ecological processes, including spatial distribution, species migration, predation process, somatic growth, species-specific reproduction, and various mortality sources, such as fishing.

### 2.1.1. Spatial distribution

Our simulated Jiaozhou Bay consists of 1435 grid cells ( $0.01^\circ \times 0.01^\circ$ ;  $35.95^\circ - 36.30^\circ \text{N}$ ;  $120.04^\circ - 120.45^\circ \text{E}$ ; Fig. 1). We assumed fish could move throughout Jiaozhou Bay. At each time step, the diffusions of fish schools follow a “random walk” process, and the range of “random walk” is set based on their swimming ability. Fish and other species were set to 2 and 1, respectively (Table A1).

### 2.1.2. Species migration

The HTL groups can be divided into (1) resident species that spend all their life stages in Jiaozhou Bay and (2) migratory species that move in and out of the simulated area (Table 1). The biomass of migratory species was set to zero at time steps corresponding to migrating out of the simulated area. The timing of migration is set based on survey data and relevant references (Table A1). The flux of species biomass ( $Bio_{flux}$ ) migrating into Jiaozhou Bay was estimated from the model calibration. Each age class for  $Bio_{flux}$  is assumed to be uniform.

### 2.1.3. Predation process

The model assumes size-based opportunistic predation processes (Shin and Cury, 2004). Prey availability is dependent on the prey-predator size ratio and spatio-temporal co-occurrence of prey and predators in the same cell at a given time step. The minimum and maximum prey-predator size ratios were set based on stomach content analysis and relevant studies (Table A1).

### 2.1.4. Somatic growth

The somatic growth of individuals is based on the amount of food obtained in predation processes. Individuals grow after ingesting enough food at a given time step. Alternatively, they stop growing or

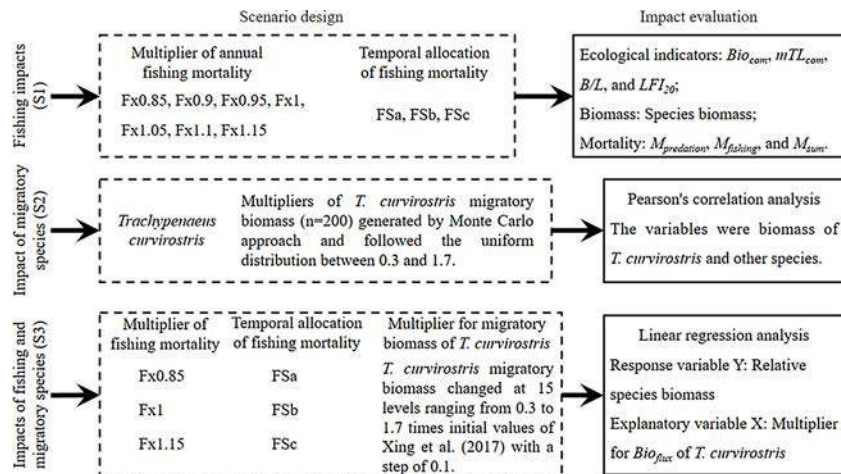


**Fig. 2.** Flow chart of the processes for simulation design. The processes of scenario design and impact evaluation are marked with dotted rectangles and solid rectangles, respectively.

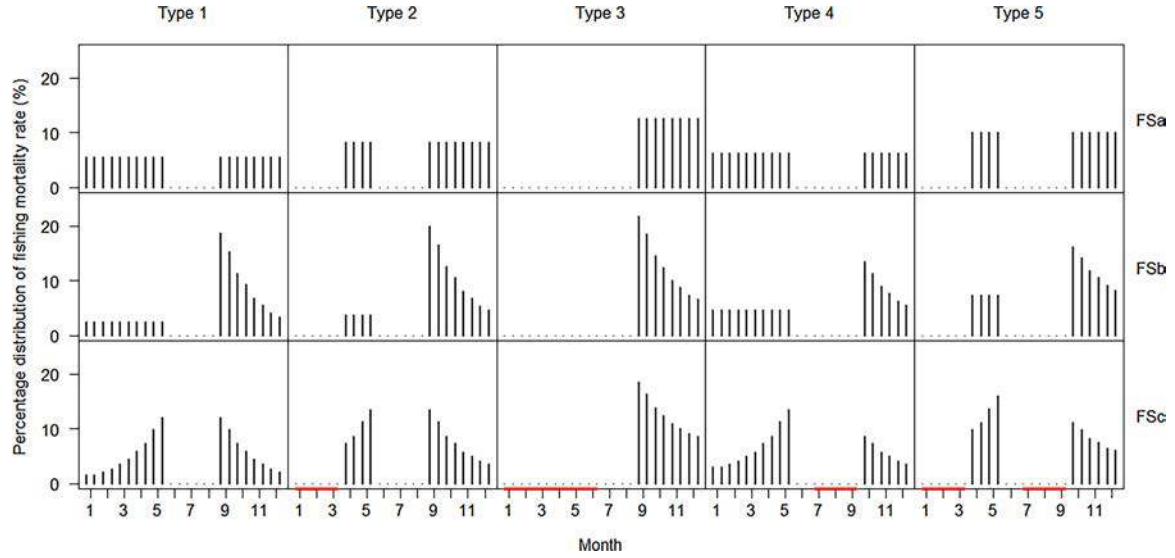


**Fig. 3.** Percentage distribution of fishing mortality rate for HTL groups. HTL groups were divided into five types based on the time migrating into/out of Jiaozhou Bay (Table 1). The sum of percentages for each HTL group in a simulated year was equal to 100 %. FSc, FSB, and FSA correspond to managing species under uniform fishing mortality, large catches landing immediately after the end of the seasonal fishing closure, and large catches landing at the start and end of the fishing season, respectively. The fishing mortality rate of one HTL group was set to zero during seasonal fishing closure or when they migrated out of Jiaozhou Bay. Type 1 refers to species that occur in the modeled area year round, including *O. oratoria* (SP0), small shrimp (SP1), *Octopus* sp. (SP5), *S. schlegelii* (SP6), *A. hexanema* (SP8), *J. belangerii* (SP11), and *C. joyneri* (SP13). Types 2 to 5 are species that migrate out of the modeled area at a given time. Type 2 includes *C. bimaculata* (SP2), *Loligo* sp. (SP4), and *T. kammalensis* (SP9). Type 3 includes *C. japonica* (SP3) and *T. curvirostris* (SP12). Types 4 and 5 include *P. fangi* (SP7) and *L. tanakae* (SP10), respectively. Time steps for moving out of the simulated domain are found in Table 1 and marked with red lines on the X axis.

starve due to the lack of food. The maximum ingestion rate, set to 3.5 g of food per gram of body weight per year, is used to define the upper limitation of food intake (Shin and Cury, 2004). The critical predation efficiency  $\xi_{crit}$ , which is equal to 0.57, determines whether individuals ingest enough food to support somatic growth (Shin and Cury, 2004). If predation efficiency  $\xi$  is higher than  $\xi_{crit}$  the growth of individuals is calculated by the von Bertalanffy model. The weight-length relationship formula calculates the individual weight at a given size (Table A1).

#### 2.1.5. Species-specific reproduction

The model considers the species-specific seasonality of reproduction. The number of eggs spawned in the spawning season is related to spawning stock biomass and relative fecundity. No eggs are produced outside of the spawning season. The spawning stock refers to individuals larger than the minimum maturity size in the spawning season. Each species' spawning season and maturity size were derived from relevant studies (Table A1).

#### 2.1.6. Various mortality sources

The five mortality sources included in the model are predation mortality ( $M_{predation}$ ), starvation mortality ( $M_{starvation}$ ), fishing mortality ( $M_{fishing}$ ), larval mortality ( $M_{larval}$ ), and additional natural mortality ( $M_{natural}$ ). Each mortality source is calculated based on a stochastic mortality algorithm in which five mortalities compete with each other.  $M_{predation}$  and  $M_{starvation}$  are related to the predation processes and calculated by the model instead of being assigned to invariant values. Additional natural mortality ( $M_{natural}$ ) represents the sum of mortality sources that are not explicitly represented in the OSMOSE model. Larval mortality ( $M_{larval}$ ) is the sum of the mortality of non-fertilization and export of eggs and first feeding larvae.

The seasonal fishing closure from Jun. 1st to Sep. 1st was considered. No catches occur during the period of closed fishing. The minimum catch size is set to 5 cm so that only individuals larger than the minimum

catch size will be harvested during the fishing season. Fishing mortality rates of HTL groups are assumed to be uniform over the fishing season. The partial parameters and equations are summarized in Appendix A.

The unknown parameters, which cannot be directly obtained from survey data and relevant studies, are estimated from the model calibration by fitting the simulated species biomass to observed survey data collected in 2011. An evolutionary algorithm (EA) was employed to find the optimal combination of unknown parameter values (Oliveros-Ramos et al., 2017). There were five types of unknown parameters: the proportion of available biomass of LTL groups to HTL groups ( $Plank.access$ ), flux of migratory species biomass ( $Bio_{flux}$ ), species-specific relative fecundity ( $RF$ ), larval mortality ( $M_{larval}$ ), and annual fishing mortality ( $M_{fishing}$ ). The unknown parameters were estimated within a reasonable range at the initiation of model calibration. Model calibration was hierarchical and estimated the parameters sequentially along the three phases:  $Plank.access$  and  $Bio_{flux}$  were estimated in all phases;  $RF$  and  $M_{larval}$  were estimated in the last two phases; and  $M_{fishing}$  was estimated in the last phase. Note that the  $RF$  and  $M_{larval}$  of species that did not spawn in Jiaozhou Bay were set to null. Further details are presented in Xing et al. (2017).

#### 2.2. Simulation design

Our study focused on an input control rule that restricted fishing effort. This rule is most commonly applied to Chinese fisheries. We set the fishing mortality rate at each time step to simulate the variability in fishing intensity (i.e., annual total fishing effort) and fishing seasonality (i.e., temporal allocation of fishing effort). *Trachypenaeus curvirostris* (SP12) is a fast-growing, short-lived migratory shrimp in Jiaozhou Bay. *T. curvirostris* biomass changed greatly in the water of the south Shandong Peninsula from 2010 to 2017 (see Appendix B). Three scenarios (S1 to S3) were designed to evaluate the possible impacts of fishing and *T. curvirostris* (Fig. 2):



**Table 2**

Definitions of indicators used in the study.

| Indicator                                    | Symbol          | Description  | Source                  |
|--|-----------------|--|-------------------------|
| Total biomass of the community               | $Bio_{com}$     | $Bio_{com} = \sum_i Bio_i$ , where $Bio_i$ denotes the biomass of a given species $i$ in the simulated area.   |                         |
| Mean trophic level of the community          | $mTL_{com}$     | $mTL_{com} = \sum_i TL_i * \frac{Bio_i}{Bio_{com}}$ , where $Bio_i$ denotes the biomass of a given species $i$ ; $Bio_{com}$ indicates the total biomass of the community calculated as aforementioned computational method; $TL_i$ represents the mean trophic level of species $i$ , and its computational method was the same as in Xing et al. (2017).   | Travers et al. (2006)   |
| Inverse fishing pressure                     | $B/L$           | $B/L = \frac{Bio_{com}}{Catch_{com}}$ , where $Catch_{com}$ denotes the total catch of the community; $Bio_{com}$ indicates total biomass of the community calculated as aforementioned computational method.  | Blanchard et al. (2010) |
| Large fish index                             | $LFI_{20}$      | $LFI_{20} = \frac{Bio_{20}}{Bio_{com}}$ , where $Bio_{20}$ and $Bio_{com}$ indicate the biomass of individuals larger than 20 cm and total biomass of the community, respectively.   | Shin et al. (2005)      |
| Species biomass                              | $Bio$           | The total biomass of a given species in the simulated area.  |                         |
| Predation mortality rate                     | $M_{predation}$ | Predation mortality rate provided in outputs of the model.   |                         |
| Fishing mortality rate                       | $M_{fishing}$   | Fishing mortality rate provided in outputs of the model.   |                         |
| Sum of predation and fishing mortality rates | $M_{sum}$       | The sum of predation and fishing mortality rate provided in outputs of the model.  |                         |
| Relative indicators                          |                 | $Relative\ EI = \frac{EI_s}{EI_{ref}}$ , where $EI_s$ and $EI_{ref}$ indicate the ecological indicators predicted in the scenario $s$ and reference state, respectively;<br>$Relative\ Bio = \frac{Bio_s}{Bio_{ref}}$ , where $Bio_s$ and $Bio_{ref}$ indicate the species biomass predicted in the scenario $s$ and reference state, respectively;<br>$Relative\ M = M_s - M_{ref}$ , where $M_s$ and $M_{ref}$ indicate the mortality rates predicted in the scenario $s$ and reference state, respectively. |                         |

- (1) Scenario S1 quantified the combined effect of fishing intensity and fishing seasonality. Seven fishing intensity levels were evaluated for the HTL groups. The annual fishing mortality rate of each HTL group ranged from 0.85 to 1.15 times their initial values (Table 1) with a step of 0.05. At each level of fishing intensity, three fishing seasonality types (FSa, FSb, and FSc) were considered based on relevant studies (Zhu, 2009; Wang, 2014; Zhang Chen, et al., 2018; Zhang Fan, et al., 2018). The fishing seasonality FSa simulated the situation that the “race to fish” did not occur (i.e., uniform fishing mortality for HTL groups over the

fishing season that was the same as Xing et al. (2017)). The fishing seasonality FSb simulated the “race to fish” occurring at the beginning of the fishing season (i.e., large catches immediately after the end of the seasonal fishing closure). The fishing seasonality FSc simulated the “race to fish” occurring at the start and end of the fishing season (i.e., large catches in May and September). Fig. 3 shows the percentage distribution of the fishing mortality rate for HTL groups in a simulated year. The fishing mortality rate of each HTL group at each time step was set equal to the product of the annual fishing mortality rate and the corresponding percentage at each time step. Fishing seasonality did not change the value of the annual fishing mortality rate;

- (2) Scenario S2 investigated the responses of other species to changes in *T. curvirostris* migratory biomass. We set the flux of migratory biomass ( $Bio_{flux}$ ) to simulate the variability in *T. curvirostris* migratory biomass. The initial  $Bio_{flux}$  of *T. curvirostris* was 196.92 t (Xing et al., 2017). Given the varying nature of migratory biomass in the ecosystem, a Monte Carlo simulation approach was employed to randomly generate multipliers for the  $Bio_{flux}$  of *T. curvirostris* from the uniform distribution. The bounds of the uniform distribution and number of multipliers are presented in Fig. 2;
- (3) Scenario S3 evaluated the impact of *T. curvirostris* migratory biomass on other species under different fishing scenarios. There were 9 fishing scenarios in S3. Three levels of fishing intensity were considered: low fishing intensity (annual fishing mortality rate of each HTL group set to 0.85 times the initial values, which are shown in Table 1) (Fx0.85), current fishing intensity (annual fishing mortality rate was the same as the initial values) (Fx1), and higher fishing intensity (annual fishing mortality set to 1.15 times the initial values) (Fx1.15). Three fishing seasonality types (FSa, FSb, and FSc) were considered and set the same as those in scenario S1. The fishing mortality rate at each time step was calculated as in S1. In each fishing scenario, the  $Bio_{flux}$  of *T. curvirostris* changed at 15 levels ranging from 0.3 to 1.7 times the initial values set in Xing et al. (2017) with a step of 0.1.

Each scenario ran for a total of 120 years. To stabilize the model, all simulations had an 80-year period of burn-in under the same configuration of the initial OSMOSE-JZB model built by Xing et al. (2017). The final 40 years were used for analysis. Every simulation subscenario in S1 and S3 was repeated 100 times to account for model stochasticity. The model outputs were averaged over the 100 simulation runs. In S2, each of the above simulations was repeated 10 times to account for model stochasticity. There were a total of 2000 (200 × 10) simulations in S2. The initial OSMOSE-JZB model repeatedly ran 100 times. The outputs simulated by the model configuration of Xing et al. (2017) were used as the reference/base state representing the ecosystem of Jiaozhou Bay in 2011 to compare with other scenarios.

### 2.3. Impact evaluation

In scenario S1, we evaluated the fishing impacts at the community, population, and individual levels. The changes in the community were described by four ecological indicators: total biomass of the community ( $Bio_{com}$ ), mean trophic level of the community ( $mTL_{com}$ ), inverse fishing pressure ( $B/L$ ), and large fish index ( $LFI_{20}$ ). Species biomass ( $Bio$ ) was used to measure the stock status at the population level. *Sebastes schlegelii* and *Johnius belangerii* are slow-growing, long-lived, and high-trophic-level fishes with small populations in Jiaozhou Bay. They are usually exposed to high fishing pressure due to their high commercial value. *Amblychaeturichthys hexanema* is a small, low-trophic-level fish

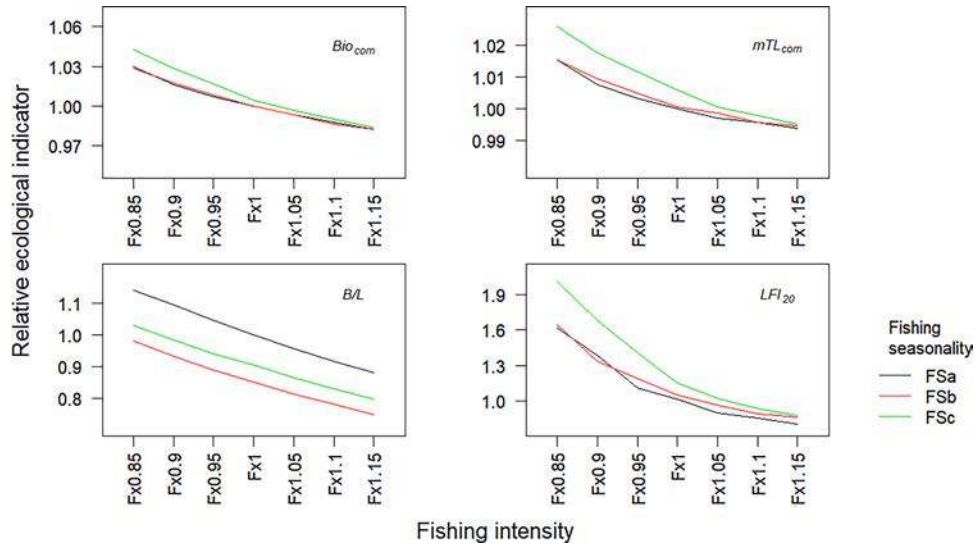


**Fig. 4.** Relative changes in ecological indicators under scenario S1. The fishing mortality rate was set from 0.85 to 1.15 times the initial values. There were three fishing seasonality types: uniform fishing mortality over the fishing season (FSa), large catches landing immediately after the end of the seasonal fishing closure (FSb), and large catches landing at the start and at the end of fishing season (FSc).

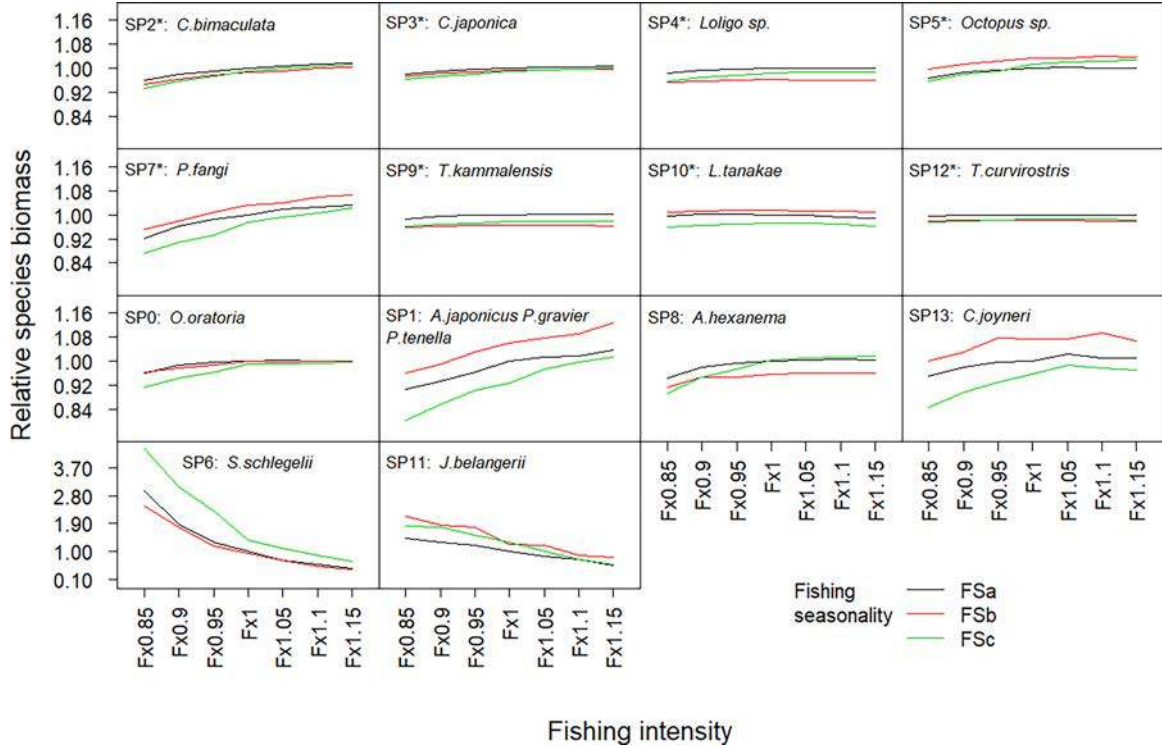


**Fig. 5.** Relative changes in species biomass under scenario S1. The fishing mortality rate was set from 0.85 to 1.15 times the initial values, and there were three fishing seasonality types (FSa, FSB, and FSc). The migratory species are marked with \*.

with abundant biomass. At the individual level, fishing ( $M_{fishing}$ ) and predation ( $M_{predation}$ ) mortality rates described the responses of individuals of two age groups (age-0 individuals who were below 1 year old and age-1 individuals who were between 1 and 2 years old) for *S. schlegelii*, *A. hexanema*, and *J. belangerii*.  $M_{predation}$  described the indirect impact of fishing, which influenced fish individuals by changing

predator pressure. The sum of predation and fishing mortality rates (i.e.,  $M_{sum}$ ) indicated the combined effect of pressure from fishing and predators.

In scenario S2, Pearson's correlation coefficient was used to test the relationship between the biomass of *T. curvirostris* and other species. In scenario S3, we used a linear regression analysis to quantify the species-

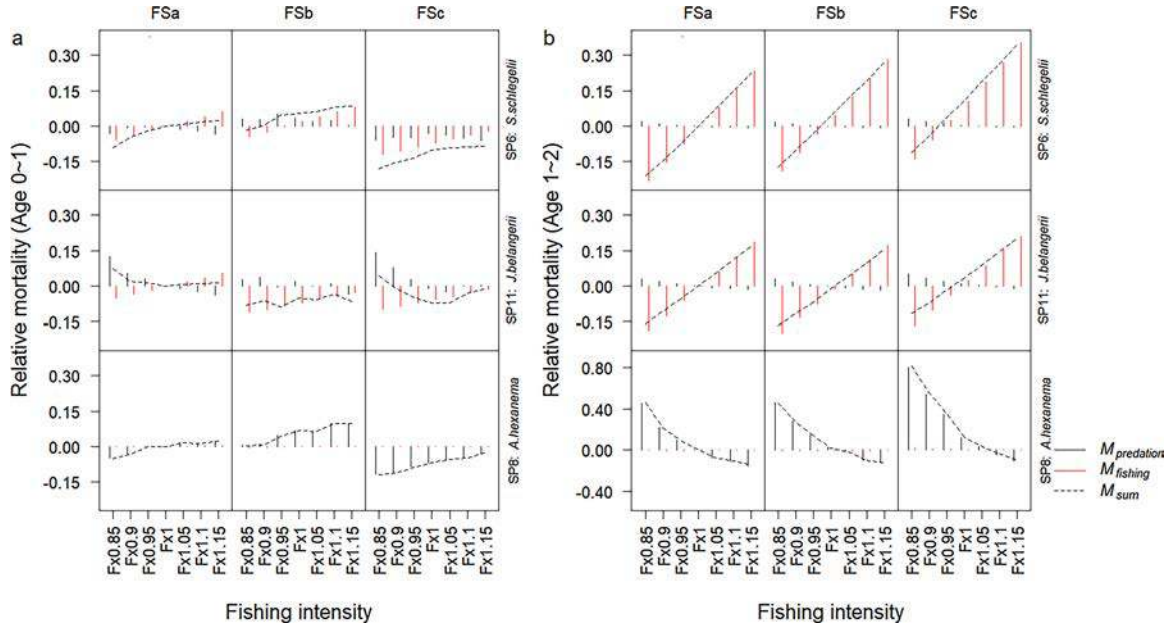


**Fig. 6.** Relative changes in predation ( $M_{predation}$ , black bars) and fishing mortality ( $M_{fishing}$ , red bars) rates for *S. schlegelii* (SP6), *J. belangerii* (SP11), and *A. hexanema* (SP8) under scenario S1. There were two age groups: individuals below 1 year old (Age-0) and individuals between 1 and 2 years old (Age-1). The indicator  $M_{sum}$  (black broken line) was the sum of relative changes in  $M_{predation}$  and  $M_{fishing}$ . The fishing mortality rate was set from 0.85 to 1.15 times the initial values, and there were three fishing seasonality types (FSa, FSB, and FSc).

**Table 3**  
Results of Pearson correlation analysis in S2.

| Type              | HTL group | Species   | Correlation coefficient (r) | P value (P) |
|-------------------|-----------|---|-----------------------------|-------------|
| Resident species  | SP0       | <i>O. oratoria</i>  | -0.901                      | <0.01       |
|                   |           | Small shrimp ( <i>P. gravieri</i> , <i>P. Tenella</i> , and <i>A. japonicus</i> ) | -0.928                      | <0.01       |
|                   | SP6       | <i>S. schlegelii</i>  | -0.643                      | <0.01       |
|                   | SP8       | <i>A. hexanema</i>  | -0.362                      | <0.01       |
|                   | SP11      | <i>J. belangerii</i>  | -0.579                      | <0.01       |
|                   | SP13      | <i>C. joyneri</i>   | -0.667                      | <0.01       |
| Migratory species | SP2*      | <i>C. bimaculata</i>  | 0.806                       | <0.01       |
|                   | SP3*      | <i>C. japonica</i>  | 0.953                       | <0.01       |
|                   | SP4*      | <i>Loligo</i> sp.   | 0.962                       | <0.01       |
|                   | SP5*      | <i>Octopus</i> sp.  | 0.785                       | <0.01       |
|                   | SP7*      | <i>P. fangi</i>   | 0.841                       | <0.01       |
|                   | SP9*      | <i>T. kammalensis</i>   | 0.839                       | <0.01       |
|                   | SP10*     | <i>L. tanakae</i>   | 0.426                       | <0.01       |

specific response to the variability of *T. curvirostris* biomass under different fishing scenarios (Halouani et al., 2019). There were 9 linear regression models for each species in S3. The formula of the linear regression model is:

$$Relative\ Bio = \frac{Bio_{sp,s}}{Bio_{sp,ref}} \quad (1)$$

$$Relative\ Bio = a \times Multiplier + b \quad (2)$$

where *Relative Bio* is the ratio of species biomass in scenario *s* ( $Bio_{sp,s}$ ) and that in the reference state ( $Bio_{sp,ref}$ ); *Multiplier* is the ratio of migratory biomass of *T. curvirostris* in scenario *s* and the reference state; and *a* and *b* are the slope and intercept in the linear regression model, respectively. The slope represented the increasing impact rate of varying *T. curvirostris* biomass under different fishing scenarios. The *P*-value determined the goodness-of-fit for the linear regression model. The indicators used in the study are shown in Table 2.

### 3. Results

#### 3.1. Fishing impacts

In general, fishing intensity had a negative relationship with the four ecological indicators (Fig. 4). The relative changes in  $Bio_{com}$  and  $mTL_{com}$  were smaller than those in  $B/L$  and  $LFI_{20}$ .  $B/L$  was highest when fishing mortality was uniform over the fishing season (FSa) and lowest when large catches landed immediately after the end of the seasonal fishing closure (FSb).  $LFI_{20}$  was highest with large catches at the beginning and end of fishing seasons (FSc).  $LFI_{20}$  had a greater increase under FSc after reducing fishing intensity (Fig. 4).

The changes in fishing seasonality altered the impact of fishing intensity on different species (Fig. 5). Except for *Pholis fangi*, migratory species had smaller changes than resident species when fishing intensity and fishing seasonality changed. The biomass of *Oratosquilla oratoria* and *A. hexanema* declined when fishing mortality was below the reference state. *A. hexanema* biomass was low under FSB. Small shrimp, *P. fangi*, and *Cynoglossus joyneri* biomasses were highest under FSB and lowest under FSc. *S. schlegelii* and *J. belangerii* were subject to changes in fishing intensity. In contrast to most species, the biomass of *S. schlegelii* and *J. belangerii* declined with increasing fishing mortality. *S. schlegelii* biomass was high under FSc, and *J. belangerii* biomass was high under FSB. Fishing seasonality had a larger impact on *S. schlegelii* and *J. belangerii* under low fishing pressure levels (Fig. 5).

The fishing intensity and fishing seasonality could alter trophic interactions (Fig. 6). The  $M_{predation}$  and  $M_{fishing}$  of age-0 *S. schlegelii* were lower under FSc than under FSa and FSB. At a low fishing pressure level (Fx0.85), age-0 *J. belangerii* underwent high predation mortality under FSa and FSc. In contrast to *S. schlegelii* and *J. belangerii*, the  $M_{fishing}$  of age-0 *A. hexanema* showed small changes. The  $M_{sum}$  of *S. schlegelii* and *A. hexanema* below 1 year old was low under FSc. The  $M_{sum}$  of age-0 *J. belangerii* was low under FSB (Fig. 6a). The  $M_{predation}$  of *S. schlegelii* and *J. belangerii* between 1 and 2 years old showed small changes in response to changes in fishing intensity and seasonality. The  $M_{predation}$  of age-1 *A. hexanema* declined after increasing fishing intensity. The  $M_{fishing}$  of age-1 *S. schlegelii* was higher under FSc than under the other two fishing seasonality types. The  $M_{predation}$  of age-1 *A. hexanema* declined



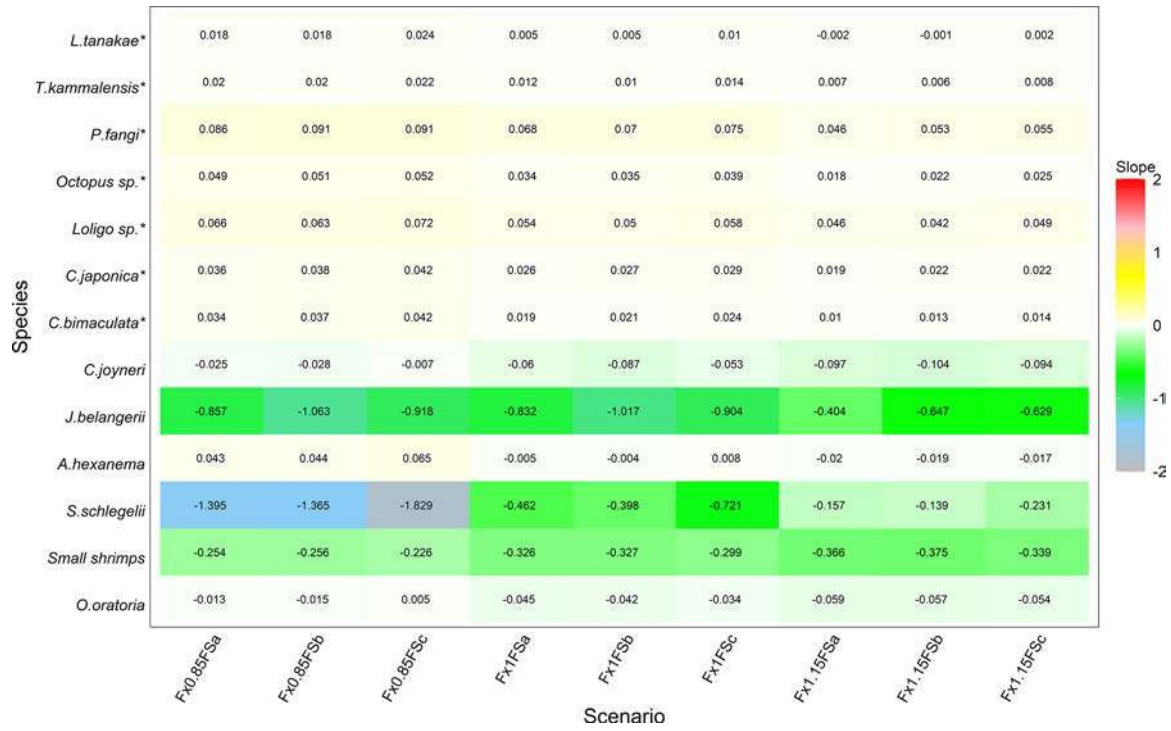


Fig. 7. Linear regression model of the relative biomass of species except for *T. curvirostris* and the corresponding multiplier. The slope values are shown in the figure and indicated by the colors. The  $P$  and  $R^2$  are shown in Fig. C.1 to Fig. C.3. The migratory species are marked with \*.

with increasing the fishing mortality of all species. The  $M_{predation}$  of age-1 *A. hexanema* under FSc was higher than that under the other two fishing seasonality types (Fig. 6b).

### 3.2. Impacts of migratory species

Pearson's correlation analysis showed that *T. curvirostris* biomass had negative correlations with resident species biomass and positive correlations with migratory species biomass (Table 3). Except for *Liparis tanakae*, the correlation coefficient values for migratory species were higher than 0.75. The correlation coefficient values of *O. oratoria* and small shrimp ( $r < -0.9$ ) were much lower than those of other resident species. It indicated that their biomass had strong negative relationships with *T. curvirostris* biomass. The correlation coefficient values of *S. schlegelii*, *J. belangerii*, and *C. joyneri* were lower than that of *A. hexanema*. The absolute value of the correlation coefficient for *A. hexanema* was lowest, indicating a weaker relationship between *A. hexanema* biomass and *T. curvirostris* biomass compared to other species (Table 3).

### 3.3. Impacts of migratory species under different fishing scenarios

The absolute values of slopes for *O. oratoria*, *A. hexanema*, *C. joyneri*, and 8 migratory species were lower than 0.1, suggesting that changes in *T. curvirostris* biomass had small impacts on these species (Fig. 7). The increase of *T. curvirostris* biomass had negative impacts on small shrimp, *S. schlegelii*, and *J. belangerii* (Slope  $< 0$ ). The slopes of *S. schlegelii* and *J. belangerii* were lower than those of small shrimp, suggesting that changes in *T. curvirostris* biomass had larger impacts on *S. schlegelii* and *J. belangerii*. The slopes of small shrimp were high under low fishing pressure. In contrast, the slopes of *S. schlegelii* and *J. belangerii* declined after reducing fishing intensity. In terms of fishing seasonality, the slopes of *S. schlegelii* and *J. belangerii* were low under FSc and FSB, respectively. The slopes of small shrimp had small changes when the fishing seasonality changed (Fig. 7).

## 4. Discussion

Heavy fishing will result in the decline of large predatory fishes and the increase of small pelagic fishes (Szuwalski et al., 2017). The S1 results highlighted the importance of managing the fishing effort to protect large fishes. Han et al. (2018) demonstrated that small fishes had an advantage against large fishes under high fishing pressure. Similarly, we found that the proportion of individuals larger than 20 cm (i.e.,  $LFI_{20}$ ) declined after increasing fishing intensity (Fig. 4). Two large resident fishes (*S. schlegelii* and *J. belangerii*) were more sensitive to fishing changes than low-trophic-level species (Fig. 5). The low-trophic-level species biomass decreased after reducing the fishing pressure to all species (Fig. 5). This result suggested that changes in trophic interactions had larger impacts on low-trophic-level species than fishing. Fishing can indirectly influence fish stocks by changing trophic interactions (Lynam et al., 2017). In our study, trophic interactions more strongly changed *A. hexanema* predation mortality (i.e.,  $M_{predation}$ ) compared to fishing mortality (Fig. 6). This result suggested that *A. hexanema* was more sensitive to changes in trophic interactions than the direct impact of fishing. Fishing changes had larger impacts on age-1 individuals for *S. schlegelii* and *J. belangerii* than age-0 individuals (Fig. 6). In contrast to *A. hexanema*, the predation mortality of age-1 *S. schlegelii* and *J. belangerii* had small changes after fishing changed (Fig. 6b). This result suggested that age-1 *S. schlegelii* and *J. belangerii* had an advantage in competing with other species.

Da-Rocha et al. (2014) advocated for the management approach of landing large catches in a short time period to let the stock grow over a longer timeframe. Other work suggests that "race to fish" (i.e., harvesting a lot in a short time period) may erode the recruitment of fish stocks (Wang et al., 2015).  $Bio_{com}$ ,  $mTL_{com}$ , and  $LFI_{20}$  were highest when the "race to fish" occurred at the start and end of the fishing season (i.e., FSc) (Fig. 4). The "race to fish" seemed to be a potential option to mitigate negative fishing impacts compared to managing fish stocks under uniform fishing pressure (i.e., FSA). At a high fishing intensity level, we noted a convergence of ecological indicators (e.g.,  $Bio_{com}$ ,  $mTL_{com}$ , and  $LFI_{20}$ ) under three fishing seasonality types (Fig. 4). This

result suggested that high fishing intensity might undermine the effectiveness of managing fishing seasonality. Past work suggested that the growth of individuals below 1 year old could influence the stocks of *S. schlegelii* and *J. belangerii* (Xing et al., 2020a). The “race to fish” that occurred at the beginning of the fishing season (i.e., FSB) favored the growth of age-0 *J. belangerii* (Fig. 6a). The *J. belangerii* biomass was highest under the fishing seasonality FSB (Fig. 5). The fishing seasonality FSc was more beneficial to age-0 *S. schlegelii*, in which the pressure of fishing and predators was low (Fig. 6a). The *S. schlegelii* biomass was high under the fishing seasonality FSc (Fig. 5). SSFs in China nearly always target multiple species. Seemingly, ideal harvest strategies will be species-specific and fishery-dependent. We note it is a significant challenge to balance optimized harvest strategies for different species simultaneously.

Migratory species can influence local marine ecosystems via trophic interactions (Mariani et al., 2017). Han et al. (2017) reported that a large number of *T. curvirostris* will add additional trophic competition with *O. oratoria* and small shrimp. Similarly, the S2 results showed that *T. curvirostris* had strong negative correlations with *O. oratoria* and small shrimp ( $r < -0.9$ ) (Table 3). Moreover, Pearson’s correlation analysis showed that increasing *T. curvirostris* biomass had negative impacts on resident species ( $r < 0$ ) and positive impacts on migratory species ( $r > 0$ ) (Table 3). This implied the competition between resident species and migratory species. The changes in *T. curvirostris* migratory biomass might present additional challenges for SSFs management. The S3 results showed that small shrimp, *S. schlegelii*, and *J. belangerii* were more sensitive to changes in *T. curvirostris* biomass than other species (Fig. 7). Moreover, fishing could influence their responses to changes in the migratory biomass of *T. curvirostris*. *T. curvirostris* had a larger impact on small shrimp under high fishing pressure. Fishing seasonality did not seem to influence the impact of *T. curvirostris* on small shrimp. The impacts of *T. curvirostris* on *S. schlegelii* and *J. belangerii* were larger under low fishing pressure. At the same fishing pressure, *S. schlegelii* was more sensitive to changes in *T. curvirostris* biomass under FSc, while *J. belangerii* was more sensitive to changes in *T. curvirostris* biomass under FSB. The compound effect of fishing and *T. curvirostris* migratory biomass further complicated SSFs management in Jiaozhou Bay.

SSFs management in China has become complicated in recent years. Except for the summer fishing moratorium, there are no specific management policies to control the temporal allocation of fishing effort during the fishing season. Such policies result in a “race to fish” each year following the lifting of the summer moratorium. Nationally, “double control” and fishing license systems are designed to restrict fishing effort (Shen and Heino, 2014). Emerging from resource instability, “fishing less” and “fishing more” are potentially adaptive strategies by fishermen in response to resource decline (Cinner et al., 2011). On the one hand, fisheries resource decline may decrease fishing effort due to increased costs and reduced catch. On the other hand, available fuel subsidies and growing market demand (i.e., price incentives) can incentivize fishermen to take more fishing trips amidst a declining resource (Mallory, 2016). Such behaviors certainly introduce uncertainty into the effectiveness of the Chinese seasonal fishing closure, “double control”, and fishing license systems.

Our findings highlight the importance of incorporating the temporal distribution of fishing effort into the decision-making process. No temporal allocation of fishing effort was beneficial to all species. Balancing the relationship between focal species and other ecological components is a challenge for SSFs management. There are increasing reports of variations in stocks of migratory shrimp and cephalopods in Chinese waters, which are fast-growing and short-lived species (Lv, 2018; Pang et al., 2018; Wu et al., 2018). The study demonstrated that the compound effects of fishing and migratory species on the local ecosystem are non-stationary and complex. We recommend that the impact of migratory species should be considered in fisheries management, especially when migratory movement has or is predicted to markedly change.

Additional aspects need to be considered when this approach is used

to inform fisheries management. The behaviors of migratory species are subject to environmental changes such as sea temperature anomalies. In addition to focusing on variations in *T. curvirostris* biomass migrating into Jiaozhou Bay, it is necessary to investigate the impacts caused by changes in migration timing. Migratory species have different responses to environmental variability, and future studies should quantify how varying the biomass of multiple migratory species influences food web stability. We recommend further cooperation between our approach and others. For example, generalized additive models and habitat suitability indices are commonly used to investigate the relationship between biomass and environmental factors (Grüss et al., 2018; Zeng et al., 2018). Incorporating species distribution models into our model is a future research direction that will improve the realism of our simulations. We have investigated the impacts of imprecise parameters, such as mortality rates and relative fecundity, on the model performance (Xing et al., 2020b). As fishing and climate change can influence individual growth rates (Martino et al., 2019), there is a need to evaluate the impacts of changing parameter values in growth sub-models.

In this study, we quantified the species-specific response to variations in fishing and migratory species biomass. In addition to controlling fishing intensity, we found that the effectiveness of recovering large predatory species can be improved by managing the “race to fish”. Managing fish stocks under uniform fishing pressure may be less effective because the exploitation (high  $B/L$ ) and community biomass (low  $B_{com}$ ) are low. Fishing can influence the impacts of migratory species on resident species. The study provides some insights into managing SSFs in China. The modeling approach can help identify potential win-win management strategies that consider both ecosystem conservation and economic profit. Although some of our conclusions may be similar to other studies and the results are based on a particular ecosystem, the approach can be applied to other small-scale fisheries ecosystems to promote ecosystem-based management of fisheries resources.

#### CRedit authorship contribution statement

**Lei Xing:** Conceptualization, Data curation, Formal analysis, Methodology, Software, Writing - original draft. **Yong Chen:** Conceptualization, Methodology, Supervision, Writing - review & editing. **Robert Boenish:** Methodology, Writing - review & editing. **Kisei R. Tanaka:** Methodology, Writing - review & editing. **Nicolas Barrier:** Methodology, Software. **Yiping Ren:** Data curation, Supervision, Funding acquisition.

#### Declaration of Competing Interest

The authors report no declarations of interest.

#### Acknowledgements

This work was funded by Marine S & T Fund of Shandong Province for Pilot National Laboratory for Marine Science and Technology (Qingdao) (No. 2018SDKJ0501-2) and National Key R&D Program of China (2018YFD0900904, 2018YFD0900906). The computational simulation and data analysis were primarily done at Dr. Chen’s lab at the University of Maine and supported by the China Scholarship Council, Ocean University of China, and University of Maine. We are extremely grateful to members of Dr. Ren’s lab at the Ocean University of China for generously providing data. The authors are grateful to Dr. Punt (Editor) and two anonymous peer reviewers for helpful comments, suggestions, and edits.

#### Appendix A. Summary of parameterization for ecological processes

**Table A1**  
Summary of equations and partial parameters modeled in the OSMOSE-JZB model built by Xing et al. (2017).

| Process              | Description of provisos and equations   | Details of partial parameters   |
|----------------------|---|---|
| Spatial distribution | “Random walk” is employed by the model for mimicking species diffusion during foraging. The range of “Random walk” determines number of adjacent cells which can be used for a given species.   | The range of random foraging was set based on their swimming ability. Seven fishes were set to 2, and other species were set to 1.  |
| Migration            | The species, which migrate into the simulated area, are characterized by biomass, age, and length. The flux of species biomass ( $B_{ioflux}$ ) migrating into Jiaozhou Bay for each age class are uniform. The model allows for setting the timing of species migration. The migratory species will be removed when they migrate out of the simulated domain.  | Time steps for moving out of simulated domain were showed in Table 1. References for species-specific migration were listed in Table B.2 of Xing et al. (2017).<br>The $B_{ioflux}$ of each species was estimated from the model calibration. Their values were listed in Table A.3 of Xing et al. (2017).  |
| Predation            | Proviso for biomass of available prey to predator (Xing et al., 2017):<br>$AP_{i,x,y,t} = \sum_j a_{ij} B_{j,x,y,t} \mid \frac{L_i}{s_{rmax}} < L_j < \frac{L_i}{s_{rmin}}$ $\begin{cases} \text{if } AP_{i,x,y,t} > r_i B_{i,x,y,t} & PB_{i,j,at} = a_{ij} B_{j,t} * \frac{r * B_{it}}{AP_{i,x,y,t}} \\ \text{if } AP_{i,x,y,t} \leq r_i B_{i,x,y,t} & PB_{i,j,at} = a_{ij} B_{j,t} \end{cases}$ where $AP_{i,x,y,t}$ represents the total prey biomass available for school $i$ in the cell $(x, y)$ at time step $t$ , $B_{j,x,y,t}$ is the biomass of prey school $j$ in the cell $(x, y)$ at $t$ , $a_{ij}$ is the availability coefficient of prey $j$ to predator $i$ , and $s_r$ is the suitable predator-prey size ratio. $t'$ corresponds to the sequential time within a time step at which fish schools feed in a random order. $PB_{i,j,at}$ represents the biomass of school $j$ preyed upon by school $i$ ;<br>When individuals ingest enough food for, they will grow and incremental length is calculated by von Bertalanffy model (Shin and Cury, 2004):<br>$\Delta L_{s,a} = L_{\infty} s (1 - e^{-K_s(a-t_0)})$ where $a$ and $\Delta L_{s,a}$ denote the fish age and mean increase of body length of species $s$ at age $a$ , respectively. $L_{\infty}$ , $K_s$ , and $t_0$ are parameters in the von Bertalanffy model.<br>The individual weight at a given size is calculated by weight-length relationship (Shin and Cury, 2004):<br>$W_{s,ait} = c_s L_{s,ait}^{b_s}$ where $W_{s,ait}$ and $L_{s,ait}$ represent the body weight and length of school $i$ for species $s$ at age $a$ and at time step $t'$ , respectively. The $c_s$ and $b_s$ are species-specific allometry parameters. | The maximum rate of ingestion $r_i$ ( $r_{max}$ ) was set for all species to 3.5 g of food per gram of body mass per year (Shin and Cury, 2004).<br>The suitable predator-prey size ratio of each species ( $s_{rmin}$ and $s_{rmax}$ ) was listed in Table A.1 of Xing et al. (2017) and set based on relevant studies and stomach content analysis of samples collected in 2011.<br><i>Plank-access</i> represents the proportion of available biomass of LTL groups to HTL groups. <i>Plank-access</i> values were estimated from the model calibration and listed in Table A.2 of Xing et al. (2017). |
| Growth               | The predation efficiency $\xi_i$ was calculated in the predation process. The critical predation efficiency $\xi_{crit}$ , which was set to 0.57, identified whether ingested food was enough to maintain its basic metabolic rates. If $\xi_i$ was lower than 0.57, individual would starve and stop growing. Parameters of von Bertalanffy model and weight-length relationship were listed in Table 2 of Xing et al. (2017).   | The predation efficiency $\xi_i$ was calculated in the predation process. The critical predation efficiency $\xi_{crit}$ , which was set to 0.57, identified whether ingested food was enough to maintain its basic metabolic rates. If $\xi_i$ was lower than 0.57, individual would starve and stop growing. Parameters of von Bertalanffy model and weight-length relationship were listed in Table 2 of Xing et al. (2017).   |
| Reproduction         | The number of eggs spawned by sexually mature individuals at each time step within a year (Shin and Cury, 2004):<br>$Neggs_{s,t} = Ratio_{sex} * RF * SSB_{s,t} * seasonality$ where $Ratio_{sex}$ is the sex ratio, $RF$ is the relative fecundity of species $s$ , $SSB_{s,t}$ is the total biomass of sexually mature fish (larger than minimum maturity size) of species $s$ at time step $t$ , and $seasonality$ is the percentage of eggs produced at each time step within a simulated year.   | There were eight HTL groups spawning in the Jiaozhou Bay: <i>O. oratoria</i> (SP0), small shrimp (SP1), <i>C. bimaculata</i> (SP2), <i>S. schlegelii</i> (SP6), <i>P. fangi</i> (SP7), <i>A. hexanema</i> (SP8), <i>J. belangerii</i> (SP11), and <i>C. joyneri</i> (SP13).<br>$Ratio_{sex}$ values of above species were assigned to 0.5.<br>The percentage of eggs produced at each time step was set based on relevant references which were listed in Table B.1 of Xing et al. (2017).<br>$RF$ of each species was estimated from the model calibration.  |
| Mortality            | There are five mortality sources included in the model: predation mortality ( $M_{predation}$ ), starvation mortality ( $M_{starvation}$ ), fishing mortality ( $M_{fishing}$ ), larval mortality ( $M_{larval}$ ), and additional natural mortality ( $M_{natural}$ ). The starvation mortality is calculated as below (Travers-Trolet et al., 2019):<br>$M_{\xi_i} = -\frac{M_{starv} \xi_i}{\xi_{crit}} + M_{starv}$ where $M_{ij}$ and $M_{max}$ are the starvation mortality rate of fish school $i$ and maximum starvation mortality rate, respectively. $\xi_i$ and $\xi_{crit}$ are predation efficiency and critical predation efficiency, respectively.   | The minimum catch size for each HTL group was set to 5 cm. In other words, fishing mortality occurred to individuals which were larger than 5 cm.<br>$M_{smax}$ for each HTL group is set to 0.3.<br>$M_{fishing}$ and $M_{larval}$ were estimated from the model calibration.<br>The values of annual $M_{fishing}$ , $M_{larval}$ and $M_{natural}$ were presented in Table 2 of Xing et al. (2017).<br>Percentage distribution of fishing mortality rate of each HTL group at different time step was shown in Fig. 3.   |

**Appendix B. Bottom trawl survey off the south of Shandong Province from 2010 to 2017**

As a result of overfishing and environmental change, there are marked variations in natural resources in the water off the south of Shandong Province. A bottom trawl survey was conducted in each summer from 2010 to 2017 to investigate stock status (Lv, 2018). The

survey area is shown in Fig. B1. *Trachypenaeus curvirostris* is a low-trophic-level shrimp off the coast of Shandong Province. The *T. curvirostris* population had markedly changed in the last ten years (Fig. B2). The *T. curvirostris* biomass was highest in 2010 (760.5 kilotons) and lowest in 2011 (28.7 kilotons).

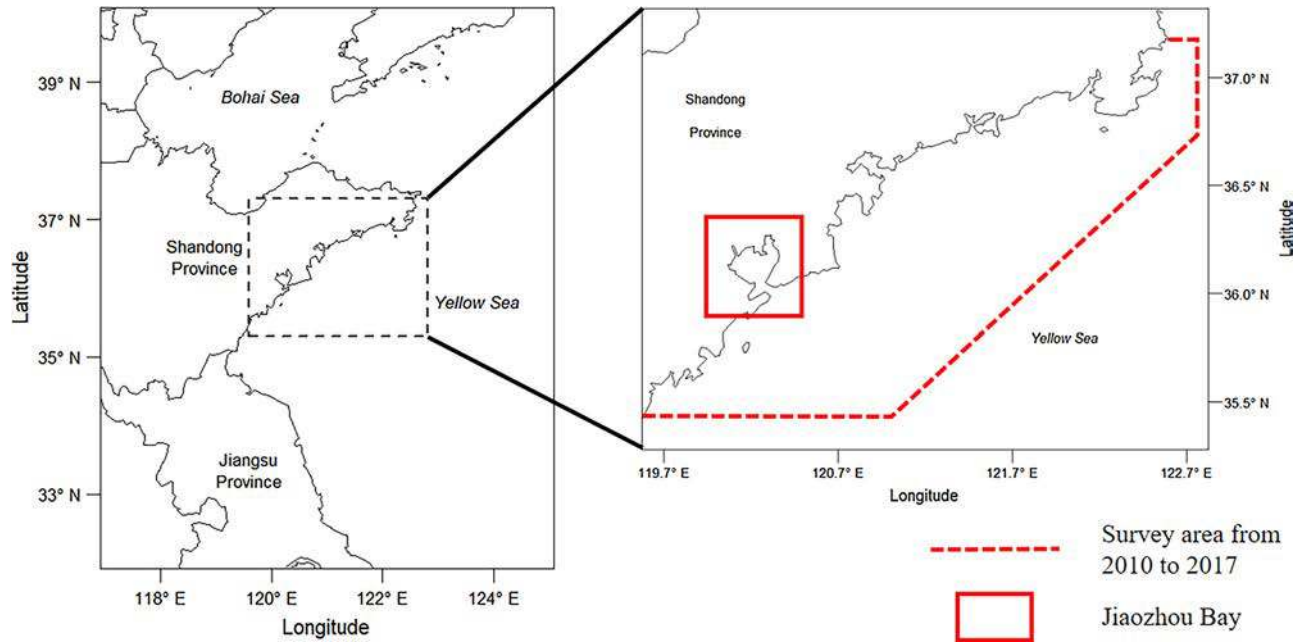


**Fig. B1.** The survey area of the bottom trawl survey off southern Shandong Province, China, from 2010 to 2017. The survey area is marked with a red dotted line in the right figure. Our study area (Jiaozhou Bay) is marked with a red rectangle.

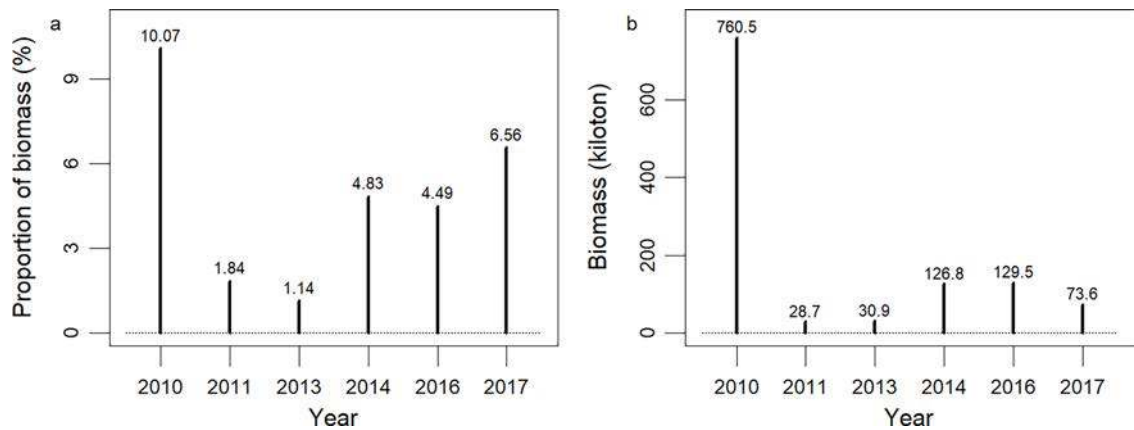


**Fig. B2.** Bottom trawl survey of *T. curvirostris* off southern Shandong Province, China, from 2010 to 2017. The proportion of *T. curvirostris* biomass in the community is summarized in the left figure (Table 5-1 of Lv, 2018). The *T. curvirostris* biomass is summarized in the right figure (Table 7-1 of Lv, 2018).

# Appendix C. Results of linear regression analysis

Figs. C1–C3

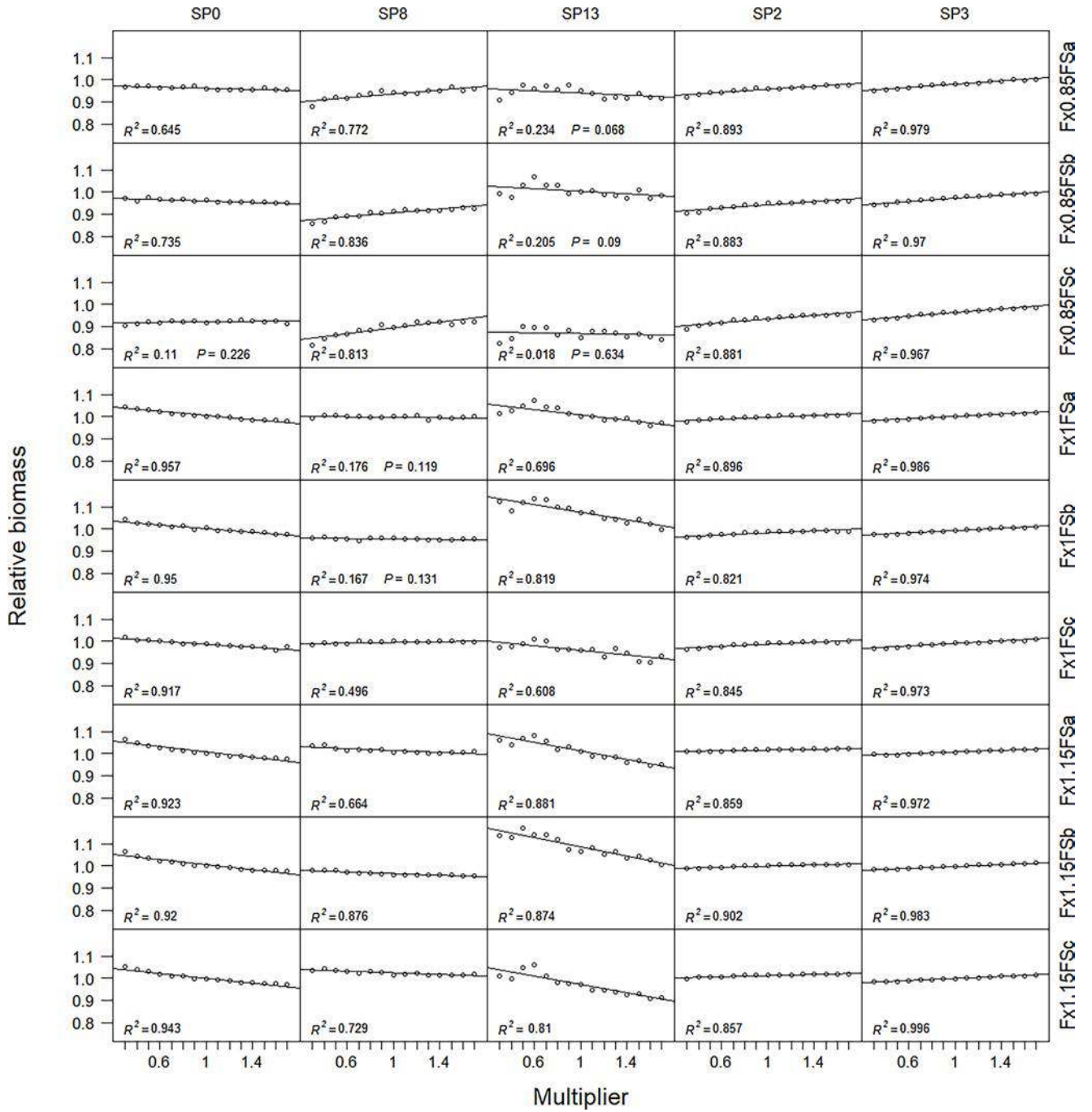


Fig. C1. Results of linear regression analysis for *O. oratoria* (SP0), *A. hexanema* (SP8), *C. joyneri* (SP13), *C. bimaculata* (SP2), and *C. japonica* (SP3) in scenario S3.  $P$  values higher than 0.05 are shown in the figure.



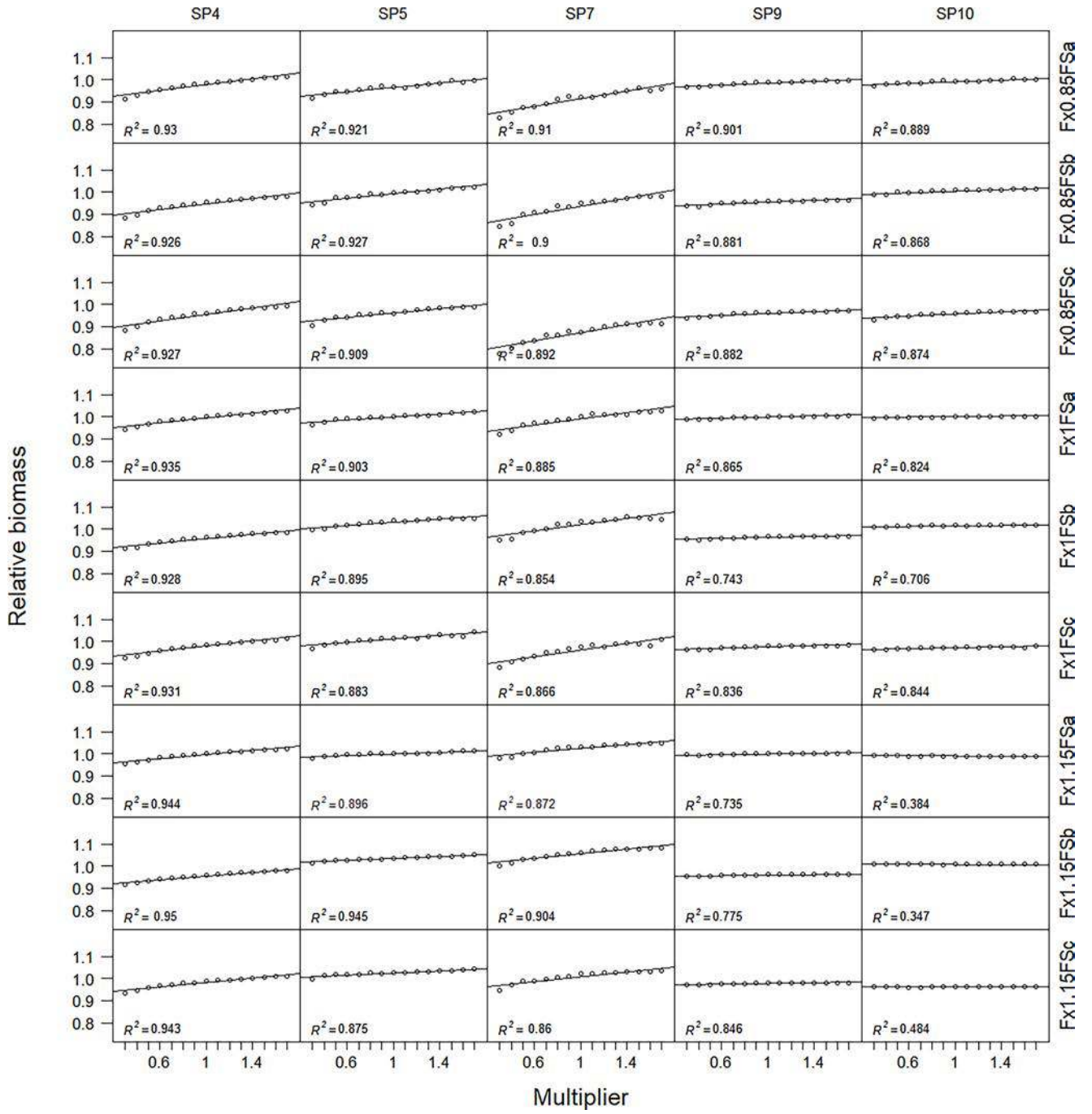
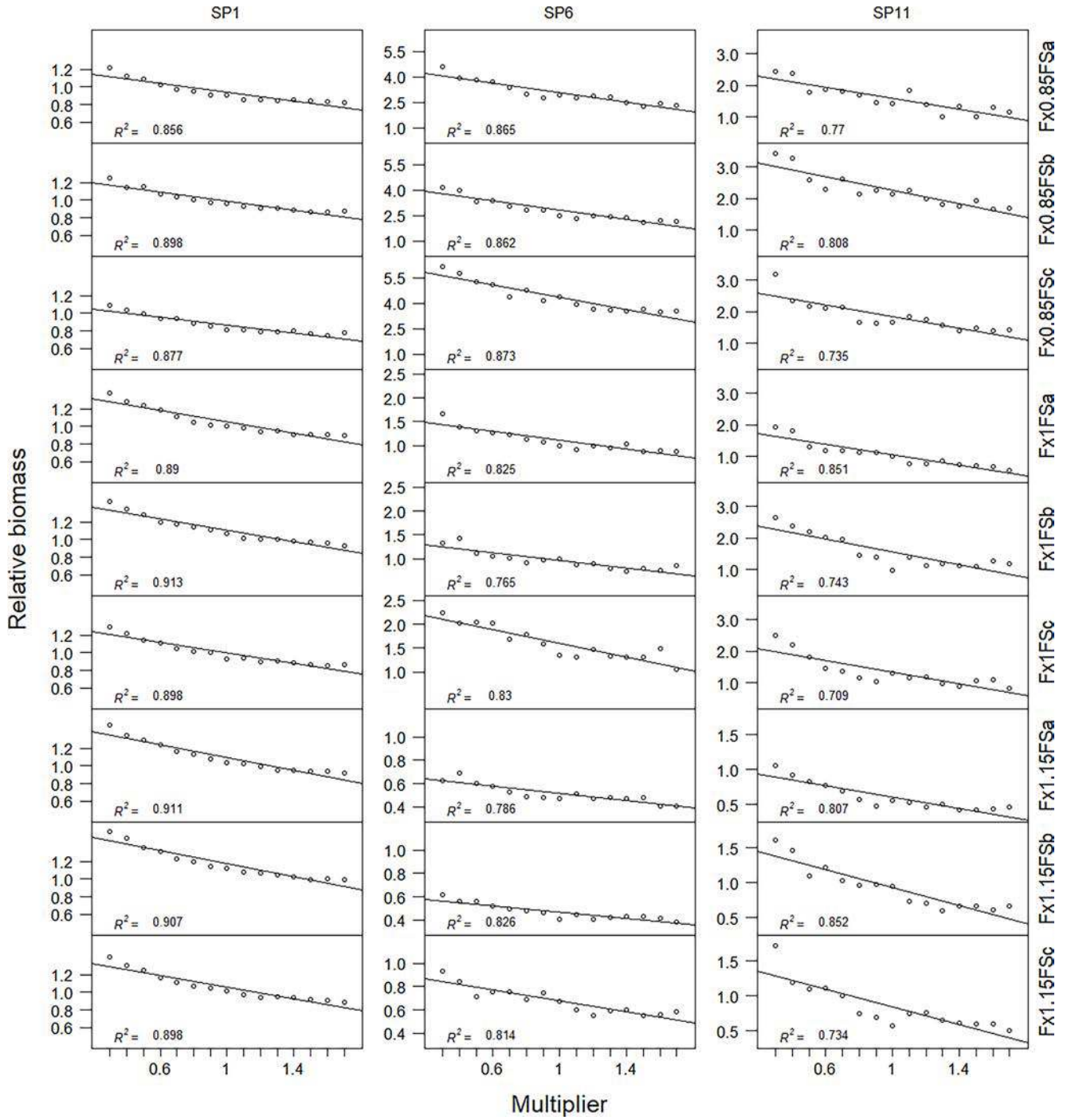


Fig. C2. Results of linear regression analysis for *Loligo* sp. (SP4), *Octopus* sp. (SP5), *P. fangi* (SP7), *T. kammalensis* (SP9), and *L. tanakae* (SP10) in scenario S3. The *P* values of these five species in the subscenarios were all lower than 0.05.



**Fig. C3.** Results of linear regression analysis for small shrimp (SP1), *S. schlegelii* (SP6), and *J. belangerii* (SP11) in scenario S3. The  $P$  values of the three fishes in the subscenarios were all lower than 0.05.

## References

- Aita, M.N., Yamanaka, Y., Kishi, M.J., 2007. Interdecadal variation of the lower trophic ecosystem in the northern Pacific between 1948 and 2002, in a 3-D implementation of the NEMURO model. *Ecol. Modell.* 202 (1-2), 81–94. <https://doi.org/10.1016/j.ecolmodel.2006.07.045>.
- Blanchard, J.L., Coll, M., Trenkel, V.M., Vergnon, R., Yemane, D., Jouffre, D., Link, J.S., Shin, Y.J., 2010. Trend analysis of indicators: a comparison of recent changes in the status of marine ecosystems around the world. *ICES J. Mar. Sci.* 67 (4), 732–744. <https://doi.org/10.1093/icesjms/isp282>.
- Chen, C., Liu, H., Beardsley, R.C., 2003. An unstructured grid, finite-volume, three-dimensional, primitive equations ocean model: application to Coastal Ocean and estuaries. *J. Atmos. Ocean. Technol.* 20 (1), 159–186. [https://doi.org/10.1175/1520-0426\(2003\)020<0159:AUGFVT>2.0.CO;2](https://doi.org/10.1175/1520-0426(2003)020<0159:AUGFVT>2.0.CO;2).
- Chen, X., Qian, S., Zhang, X., Wang, X., 2019. Bibliometric-based analysis of research progress in science of fishery resources. *Chin. Agric. Sci. Bull. (in Chinese)* 35 (31), 153–164.
- Cinner, J.E., Folke, C., Daw, T., Hicks, C.C., 2011. Responding to change: using scenarios to understand how socioeconomic factors may influence amplifying or dampening exploitation feedbacks among Tanzanian fishers. *Glob. Environ. Change* 21 (1), 7–12. <https://doi.org/10.1016/j.gloenvcha.2010.09.001>.
- Dai, Y., Wu, H., Zhang, W., Wang, J., Jiao, J., 2020. Current researching status of marine fishery ecosystem in China outlined basing on Ecopath model. *Trans. Oceanol. Limnol. (in Chinese)* 6, 150–157. <https://doi.org/10.13984/j.cnki.cn37-1141.2020.06.019>.
- Da-Rocha, J.M., Nøstbakken, L., Pérez, M., 2014. Pulse fishing and stock uncertainty. *Environ. Resour. Econ.* 59 (2), 257–274. <https://doi.org/10.1007/s10640-013-9727-y>.
- Finkbeiner, E.M., Micheli, F., Saenz-Arroyo, A., Vazquez-Vera, L., Perafan, C.A., Cárdenas, J.C., 2018. Local response to global uncertainty: insights from experimental economics in small-scale fisheries. *Glob. Environ. Change* 48, 151–157. <https://doi.org/10.1016/j.gloenvcha.2017.11.010>.
- Food and Agriculture Organisation (FAO), 2018. The State of World Fisheries and Aquaculture 2018-Meeting the Sustainable Development Goals. Rome. Licence: CCBY-NC-SA3.0IGO.
- Fulton, E.A., Smith, A.D.M., Smith, D.C., Van Putten, I.E., 2011. Human behaviour: the key source of uncertainty in fisheries management. *Fish. Fish.* 12 (1), 2–17. <https://doi.org/10.1111/j.1467-2979.2010.00371.x>.
- Gough, C.L.A., Dewar, K.M., Godley, B.J., Zafindranosy, E., Broderick, A.C., 2020. Evidence of overfishing in small-scale fisheries in Madagascar. *Front. Mar. Sci.* 7, 317. <https://doi.org/10.3389/fmars.2020.00317>.
- Grüss, A., Thorson, J.T., Babcock, E.A., Tarnecki, J.H., 2018. Producing distribution maps for informing ecosystem-based fisheries management using a comprehensive survey database and spatio-temporal models. *ICES J. Mar. Sci.* 75 (1), 158–177. <https://doi.org/10.1093/icesjms/fsx120>.
- Halouani, G., Le Loc'h, F., Shin, Y.J., Velez, L., Hattab, T., Romdhane, M.S., Lasram, F.B.R., 2019. An end-to-end model to evaluate the sensitivity of ecosystem indicators to track fishing impacts. *Ecol. Indic.* 98, 121–130. <https://doi.org/10.1016/j.ecolind.2018.10.061>.
- Han, D., Xue, Y., Zhang, C., Ren, Y., 2017. A mass balanced model of trophic structure and energy flows of a semi-closed marine ecosystem. *Acta Oceanol. Sin.* 36 (10), 60–69. <https://doi.org/10.1007/s13131-017-1071-6>.
- Han, D., Chen, Y., Zhang, C., Ren, Y., Xu, B., Xue, Y., 2018. Evaluation of effects of shellfish aquaculture and capture fishery on a semi-closed bay ecosystem. *Estuar. Coast. Shelf Sci.* 207, 175–182. <https://doi.org/10.1016/j.ecss.2018.04.005>.
- Herrón, P., Castellanos-Galindo, G.A., Stäbler, M., Díaz, J.M., Wolff, M., 2019. Toward ecosystem-based assessment and management of small-scale and multi-gear fisheries: insights from the tropical eastern Pacific. *Front. Mar. Sci.* 6, 127. <https://doi.org/10.3389/fmars.2019.00127>.
- Hilborn, R., 2011. Future directions in ecosystem based fisheries management: a personal perspective. *Fish. Res.* 108, 235–239. <https://doi.org/10.1016/j.fishres.2010.12.030>.
- Kiyama, S., Yamazaki, S., 2018. The impact of stock collapse on small-scale fishers' behavior: evidence from Japan. *Can. J. Fish. Aquat. Sci.* 75 (12), 2241–2254. <https://doi.org/10.1139/cjfas-2017-0091>.
- Lv, Y., 2018. Assessment of Important Fishery Resources in the South Offshore of Shandong from 2010 to 2017. Yantai University, China. M.s. thesis (in Chinese).
- Lynam, C.P., Llope, M., Möllmann, C., Helaouët, P., Bayliss-Brown, G.A., Stenseth, N.C., 2017. Interaction between top-down and bottom-up control in marine food webs. *Proc. Natl. Acad. Sci.* 114 (8), 1952–1957. <https://doi.org/10.1073/pnas.1621037114>.
- Ma, M., Xu, S., Xu, Y., Zhang, K., Yuan, W., Chen, Z., 2018. Comparative study of Jiaozhou Bay ecosystem based on an Ecopath model. *J. Fish. Sci. China (in Chinese)* 25 (2), 413–422. <https://doi.org/10.3724/SP.J.1118.2018.17335>.
- Mallory, T.G., 2016. Fisheries subsidies in China: quantitative and qualitative assessment of policy coherence and effectiveness. *Mar. Policy* 68, 74–82. <https://doi.org/10.1016/j.marpol.2016.01.028>.
- Mariani, P., Andersen, K.H., Lindegren, M., MacKenzie, B.R., 2017. Trophic impact of Atlantic bluefin tuna migrations in the North Sea. *ICES J. Mar. Sci.* 74 (6), 1552–1560. <https://doi.org/10.1093/icesjms/fsx027>.
- Martino, J.C., Fowler, A.J., Doubleday, Z.A., Grammer, G.L., Gillanders, B.M., 2019. Using otolith chronologies to understand long-term trends and extrinsic drivers of growth in fisheries. *Ecosphere* 10 (1), e02553. <https://doi.org/10.1002/ecs2.2553>.
- Mormul, R.P., Thomaz, S.M., Agosinho, A.A., Bonecker, C.C., Mazzeom, N., 2012. Migratory benthic fishes may induce regime shifts in a tropical floodplain pond. *Freshw. Rev.* 57 (8), 1592–1602. <https://doi.org/10.1111/j.1365-2427.2012.02820.x>.
- Moullec, F., Barrier, N., Drira, S., Guilhaumon, F., Marsaleix, P., Somot, S., Ulses, C., Velez, L., Shin, Y.J., 2019. An end-to-end model reveals losers and winners in a warming Mediterranean Sea. *Front. Mar. Sci.* 6, 345. <https://doi.org/10.3389/fmars.2019.00345>.
- Oliveros-Ramos, R., Verley, P., Echevin, V., Shin, Y.J., 2017. A sequential approach to calibrate ecosystem models with multiple time series data. *Prog. Oceanogr.* 151, 227–244. <https://doi.org/10.1016/j.pcean.2017.01.002>.
- Pang, Y., Tian, Y., Fu, C., Wang, B., Li, J., Ren, Y., Wan, R., 2018. Variability of coastal cephalopods in overexploited China Seas under climate change with implications on fisheries management. *Fish. Res.* 208, 22–33. <https://doi.org/10.1016/j.fishres.2018.07.004>.
- Pauly, D., Liang, C., 2019. The fisheries of the South China Sea: major trends since 1950. *Mar. Policy* 121, 103584. <https://doi.org/10.1016/j.marpol.2019.103584>.
- Pikitch, E.K., Santora, C., Babcock, E.A., Bakun, A., Bonfil, R., Conover, D.O., Dayton, P., Doukakis, P., Fluharty, D., Heneman, B., Houde, E.D., Link, J., Livingston, P.A., Mangel, M., McAllister, M.K., Pope, J., Sainsbury, K.J., 2004. Ecosystem-based fishery management. *Science* 305 (5682), 346–347. <https://doi.org/10.1126/science.1098222>.
- Ramírez, J.G., Leonart, J., Coll, M., Reyes, F., Puentes, G.M., 2017. Improving stock assessment and management advice for data-poor small-scale fisheries through participatory monitoring. *Fish. Res.* 190, 71–83. <https://doi.org/10.1016/j.fishres.2017.01.015>.
- Said, A., Chuenpagdee, R., 2019. Aligning the sustainable development goals to the small-scale fisheries guidelines: a case for EU fisheries governance. *Mar. Policy* 107, 103599. <https://doi.org/10.1016/j.marpol.2019.103599>.
- Salas, S., Barragan-Paladines, M.J., Chuenpagdee, R., 2019. Viability and Sustainability of Small-Scale Fisheries in Latin America and The Caribbean. Springer International Publishing, Cham, pp. 4–6. <https://doi.org/10.1007/978-3-319-76078-0>.
- Shen, G., Heino, M., 2014. An overview of marine fisheries management in China. *Mar. Policy* 44, 265–272. <https://doi.org/10.1016/j.marpol.2013.09.012>.
- Shin, Y.J., Cury, P., 2001. Exploring fish community dynamics through size-dependent trophic interactions using a spatialized individual-based model. *Aquat. Living Resour.* 14 (2), 65–80. [https://doi.org/10.1016/S0990-7440\(01\)01106-8](https://doi.org/10.1016/S0990-7440(01)01106-8).
- Shin, Y.J., Cury, P., 2004. Using an individual-based model of fish assemblages to study the response of size spectra to changes in fishing. *Can. J. Fish. Aquat. Sci.* 61 (3), 414–431. <https://doi.org/10.1139/F03-154>.
- Shin, Y.J., Rochet, M.J., Jennings, S., Field, J.G., Gislason, H., 2005. Using size-based indicators to evaluate the ecosystem effects of fishing. *ICES J. Mar. Sci.* 62 (3), 384–396. <https://doi.org/10.1016/j.jicesjms.2005.01.004>.
- Stockwell, J.D., Yule, D.L., Hrabik, T.R., Sierszen, M.E., Isaac, E.J., 2014. Habitat coupling in a large lake system: delivery of an energy subsidy by an offshore planktivore to the nearshore zone of Lake Superior. *Freshw. Rev.* 59 (6), 1197–1212. <https://doi.org/10.1111/fwb.12340>.
- Su, S., Tang, Y., Chang, B., Zhu, W., Chen, Y., 2020. Evolution of marine fisheries management in China from 1949 to 2019: How did China get here and where does China go next? *Fish. Fish.* 21 (2), 435–452. <https://doi.org/10.1111/faf.12439>.
- Sys, K., Van Meensel, J., Polet, H., Buysse, J., 2017. A temporal race-for-fish: the interplay between local hotspots of flatfish and exploitation competition between beam trawlers after a seasonal spawning closure. *Fish. Res.* 193, 21–32. <https://doi.org/10.1016/j.fishres.2017.03.018>.
- Szuwalski, C.S., Burgess, M.G., Costello, C., Gaines, S.D., 2017. High fishery catches through trophic cascades in China. *P. Natl. Acad. Sci. U. S. A.* 114 (4), 717–721. <https://doi.org/10.1073/pnas.1612722114>.
- Teh, L.C.L., Sumaila, U.R., 2013. Contribution of marine fisheries to worldwide employment. *Fish. Fish.* 14 (1), 77–88. <https://doi.org/10.1111/j.1467-2979.2011.00450.x>.
- Travers, M., Shin, Y.J., Shannon, L., Cury, P., 2006. Simulating and testing the sensitivity of ecosystem-based indicators to fishing in the Southern Benguela ecosystem. *Can. J. Fish. Aquat. Sci.* 63 (4), 943–956. <https://doi.org/10.1139/F06-003>.
- Travers-Trolet, M., Coppin, F., Cresson, P., Cugier, P., Oliveros-Ramos, R., Verley, P., 2019. Emergence of negative trophic level-size relationships from a size-based, individual-based multispecies fish model. *Ecol. Modell.* 410, 108800. <https://doi.org/10.1016/j.ecolmodel.2019.108800>.
- Wang, X., 2013. A Strategic Study on Development of Marine Ecology Fishery in Blue Economic Area of Shandong Peninsular. Ocean University of China, China. Ph.D. thesis (in Chinese).
- Wang, Y., 2014. The Analysis on Trajectory Simulation of Single Otter Trawl Vessels and Its Production Estimates As Well as Spatio-Temporal Characteristics in Zhoushan Fishing Ground in Autumn and Winter. Zhejiang Ocean University, China. M.s. thesis (in Chinese).
- Wang, Y., Duan, L., Li, S., Zeng, Z., Failler, P., 2015. Modeling the effect of the seasonal fishing moratorium on the Pearl River Estuary using ecosystem simulation. *Ecol. Modell.* 312, 406–416. <https://doi.org/10.1016/j.ecolmodel.2015.06.011>.
- Wu, Q., Li, Z., Wang, J., Shan, X., Jin, X., 2018. Inter-annual variation in the community structure of crustaceans in the Bohai Sea during summer. *Progr. Fish. Sci.* 39 (2), 16–23. <https://doi.org/10.19663/j.issn2095-9869.20171111001>.
- Xing, L., Zhang, C., Chen, Y., Shin, Y.J., Verley, P., Yu, H., Ren, Y., 2017. An individual-based model for simulating the ecosystem dynamics of Jiaozhou Bay, China. *Ecol. Modell.* 360, 120–131. <https://doi.org/10.1016/j.ecolmodel.2017.06.010>.
- Xing, L., Chen, Y., Zhang, C., Li, B., Shin, Y.J., Ren, Y., 2020a. Evaluating impacts of pulse fishing on the effectiveness of seasonal closure. *Acta Oceanol. Sin.* 39 (4), 89–99. <https://doi.org/10.1007/s13131-020-1536-x>.
- Xing, L., Chen, Y., Zhang, C., Li, B., Tanaka, K.R., Boenish, R., Ren, Y., 2020b. Evaluating impacts of imprecise parameters on the performance of an ecosystem model

- OSMOSE-JZB. Ecol. Modell. 419, 108923 <https://doi.org/10.1016/j.ecolmodel.2019.108923>.
- Xu, S., Guo, J., Chen, Z., Zhang, K., Xu, Y., Cai, Y., Li, C., 2019. Tempo-spatial distribution characteristics of fish resources in Jiaozhou Bay. J. Fish. China (in Chinese) 43 (7), 1615–1625. <https://doi.org/10.11964/jfc.20180911461>.
- Yang, H., 2019. Development ideas and implementation approaches of blue granary scientific and technological innovation in China. J. Fish. China (in Chinese) 43 (1), 97–104. <https://doi.org/10.11964/jfc.20181211596>.
- Yuan, X., Liu, Z., Cheng, J., Tian, Y., 2017. Impact of climate change on nekton community structure and some commercial species in the offshore area of the northern East China Sea in winter. Acta Ecol. Sin. (in Chinese) 37 (8), 2796–2808. <https://doi.org/10.5846/stxb201512222549>.
- Zeng, X., Tanaka, K.R., Chen, Y., Wang, K., Zhang, S., 2018. Gillnet data enhance performance of rockfishes habitat suitability index model derived from bottom-trawl survey data: a case study with *Sebasticus marmoratus*. Fish. Res. 204, 189–196. <https://doi.org/10.1016/j.fishres.2018.02.009>.
- Zhang, C., Chen, Y., Ren, Y., 2016. An evaluation of implementing long-term MSY in ecosystem-based Fisheries management: incorporating trophic interaction, bycatch and uncertainty. Fish. Res. 174, 179–189. <https://doi.org/10.1016/j.fishres.2015.10.007>.
- Zhang, C., Chen, Y., Xu, B., Xue, Y., Ren, Y., 2018. Evaluating fishing effects on the stability of fish communities using a size-spectrum model. Fish. Res. 197, 123–130. <https://doi.org/10.1016/j.fishres.2017.09.004>.
- Zhang, M., Fan, W., Zhang, H., Yang, S., Tang, F., Zhu, W., 2018. Dynamic monitoring and analysis of number of fishing vessel voyages in Hainan Province based on Beidou position data. South China Fish. Sci. 14 (5), 1–10. <https://doi.org/10.3969/j.issn.2095-0780.2018.05.001>.
- Zhu, Y., 2009. Research on the Effects of China's Summer Fishing Moratorium - A Perspective of Institutional Analysis. Ocean University of China, China. Ph.D. thesis (in Chinese).